

## Research Article

# V-Band Multiport Heterodyne Receiver for High-Speed Communication Systems

Serioja O. Tatu and Emilia Moldovan

*Institut National de la Recherche Scientifique, Énergie, Matériaux et Télécommunications (INRS-EMT),  
800 de la Gauchetière Ouest, R 6900, Montréal, Canada H5A 1K6*

Received 20 April 2006; Revised 10 October 2006; Accepted 11 October 2006

Recommended by Kiyoshi Hamaguchi

A V-band receiver using a MHMIC multiport circuit is presented in this paper. The millimeterwave frequency conversion is performed using a passive circuit, the multiport, and related power detectors, avoiding the conventional millimeter-wave active costly mixers. Basically, the multiport circuit is an additive mixer in which the resulting sum of millimeter-wave signals is nonlinearly processed using millimeter-wave power detectors. This multiport heterodyne receiver is an excellent candidate for the future low-cost high-speed millimeter-wave wireless communication systems. The operating principle of the proposed heterodyne receiver and demodulation results of high-speed MPSK/QAM signals are presented and discussed in this paper. According to suggested datarate of 100–400 Mbps used to prove the operating principle, the IF of this receiver was chosen at 900 MHz. Therefore, this receiver is a possible alternative solution for WPAN applications

Copyright © 2007 S. O. Tatu and E. Moldovan. This is an open access article distributed under the Creative Commons Attribution License, which permits unrestricted use, distribution, and reproduction in any medium, provided the original work is properly cited.

## 1. INTRODUCTION

The modern communication receivers are more and more exigent in terms of wide-band, datarates, size, and costs [1]. The millimeter-wave technology has received increased attention in both academia and industry for very high-datarate wireless personal area network (WPAN) applications such as wireless data bus for cable replacement, high-speed wireless Internet access, wireless direct communication between notebooks and related devices, and wireless high-resolution TV and videoconferencing. The IEEE 802.15.3c industrial standard based on millimeter-wave technology has been recently introduced for WPAN.

The use of millimeter-wave frequencies enables the design of compact and low-cost wireless millimeter-wave communication front-ends, which can offer convenient terminal mobility and high-capacity channels. This wide range of applications requires low-cost equipment operating at hundreds of megabits per second. In the last decade initial research has been made, especially in terms of designing new millimeter wave components operating over the V-band [2–5].

In order to improve overall performances of the communication receivers, alternative wide-band architectures for

high-speed wireless communication systems have been explored in the past years [6–10].

This paper presents MPSK/QAM demodulation results of a V-band multiport heterodyne receiver suitable for very high-datarate WPAN applications.

## 2. THE MULTIPORT MIXER

The main purpose of this paper is to demonstrate that the multiport circuit together with related power detectors and two differential amplifiers can successfully replace a conventional mixer in a low-cost millimeter-wave heterodyne or homodyne architecture.

The multiport equivalent circuit of the heterodyne receiver uses four power detectors and two differential amplifiers operating at IF frequency. The multiport block diagram is shown in Figure 1. The circuit is composed of four 90° hybrid couplers and a 90° phase shifter.

Let us assume that there are two input normalized waves,  $a_5$  from the LO and  $a_6$  from the RF input, having different amplitudes and frequencies. The MPSK/QAM modulated signals can be expressed using the phase and the amplitude variation of the RF input signal,  $\alpha(t)$  and  $\varphi_6(t)$ ,

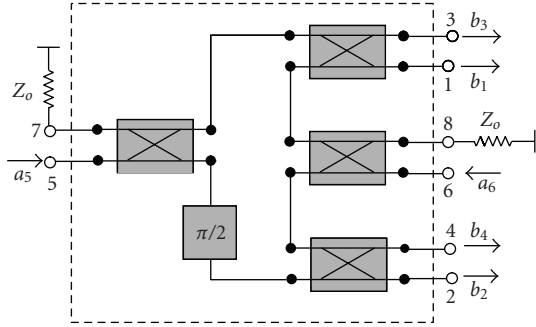


FIGURE 1: The multiport circuit block diagram.

respectively,

$$\begin{aligned} a_5 &= a \cdot \exp [j(\omega_0 \cdot t + \varphi_5)], \\ a_6 &= \alpha(t) \cdot a \cdot \exp [j(\omega \cdot t + \varphi_6(t))]. \end{aligned} \quad (1)$$

The output detected signals can be calculated based on the multiport block diagram and using the quadratic characteristic of the power detectors:

$$v_i(t) = K \cdot |b_i(t)|^2, \quad (2)$$

$$v_{1,3}(t) = K \frac{a^2}{4} \cdot \{1 + \alpha(t)^2 - / + 2 \cdot \alpha(t) \cdot \cos [-\Delta\omega \cdot t + \Delta\varphi(t)]\}, \quad (3)$$

$$v_{2,4}(t) = K \frac{a^2}{4} \cdot \{1 + \alpha(t)^2 - / + 2 \cdot \alpha(t) \cdot \sin [-\Delta\omega \cdot t + \Delta\varphi(t)]\}. \quad (4)$$

In the previous equation,  $\Delta\omega = \omega_0 - \omega$  represents the frequency difference between the multiport inputs (superheterodyne), and  $\Delta\varphi(t) = \varphi_6(t) - \varphi_5$  is the phase difference between the same signals.

Considering the sinusoidal antiphase signals in each equation (3) or (4), the DC offset is eliminated using a differential approach. Therefore the output I/Q signals are

$$\begin{aligned} i(t) &= v_3(t) - v_1(t) = K \cdot \alpha(t) \cdot |a|^2 \cdot \cos [-\Delta\omega \cdot t + \Delta\varphi(t)], \\ q(t) &= v_4(t) - v_2(t) = K \cdot \alpha(t) \cdot |a|^2 \cdot \sin [-\Delta\omega \cdot t + \Delta\varphi(t)]. \end{aligned} \quad (5)$$

The previous equations show that the multiport circuit with four power detectors and two differential amplifiers can successfully replace a conventional mixer.

Therefore the equivalence between the conventional I/Q mixer architecture and the multiport mixer, as presented in Figure 2, has been demonstrated.

It must be noted that conventional superheterodyne approach using a down-converter does not have a direct equivalence with the proposed multiport approach. This conventional receiver can be implemented using a V-band down-converter mixer (a balun and two Schottky diodes, e.g.) and a IF I/Q mixer.

In practice, for a multiport heterodyne receiver, the carrier frequency  $\omega$  is close to the local oscillator frequency  $\omega_0$ .

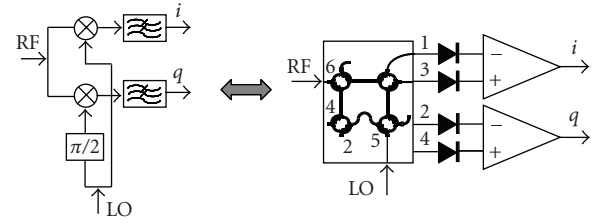


FIGURE 2: Equivalence between the conventional I/Q mixer and the multiport mixer.

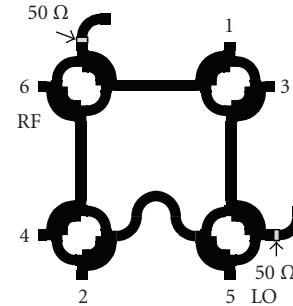


FIGURE 3: Layout of the V-band multiport circuit.

Therefore, these receivers are low IF heterodyne receivers. However, if  $\omega_0 = \omega$ , I/Q direct conversion is obtained in a homodyne architecture. This aspect can be considered as an important advantage of the proposed receiver compared to the conventional V-band down-conversion receiver. The same multiport front-end can be used for both heterodyne and homodyne architectures. In addition, signal to noise ratio is improved using a multiport circuit. The cost of additional hybrids and two Schottky diodes is compensated by the reduced cost of the IF stage (IF mixers instead of the conventional IF I/Q mixer).

A V-band multiport circuit was designed in MHEM technology using a  $125 \mu\text{m}$  ceramic substrate having a relative permittivity of 9.9. Figure 3 shows the layout of the circuit having a size of approximately 3 mm by 3 mm. The circuit is composed of four  $90^\circ$  hybrid couplers connected by  $50 \Omega$  microstrip transmission lines. In order to avoid reflections at the two unused ports of the multiport circuit, two  $50 \Omega$  loads are connected to open circuited quarter-wave transmission lines (virtual RF short-circuits). The hybrid coupler connected to LO port together with the  $90^\circ$  phase shifter (made using an additional quarter-wave transmission line on a curved branch) is equivalent to an in-phase 3 dB power divider. The circuit was optimized to operate at the 60 GHz central frequency using ADS Momentum software.

In order to obtain the four output detected signals, as expressed by (3) and (4), power detectors, composed of Schottky diodes with related matching networks, must be connected at multiport outputs. The I/Q IF signals of the proposed V-band mixer will be finally obtained using two differential amplifiers.

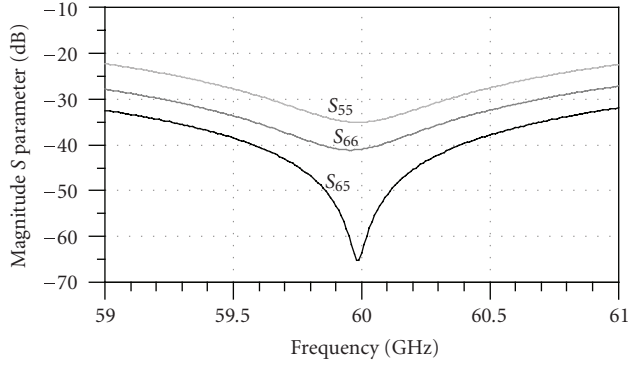


FIGURE 4: Simulation results of the return loss and isolation at RF inputs.

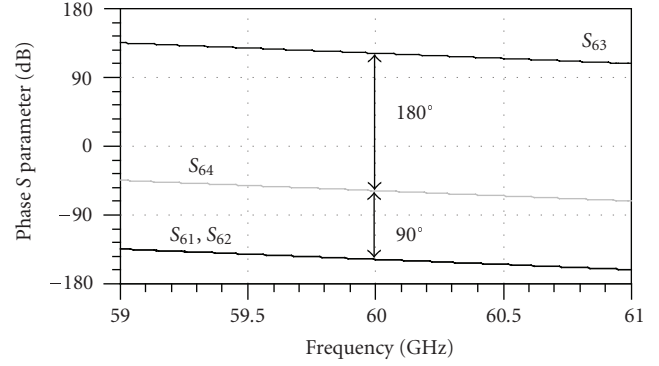


FIGURE 6: Simulation results of the transmission S parameter phase corresponding to the RF input.

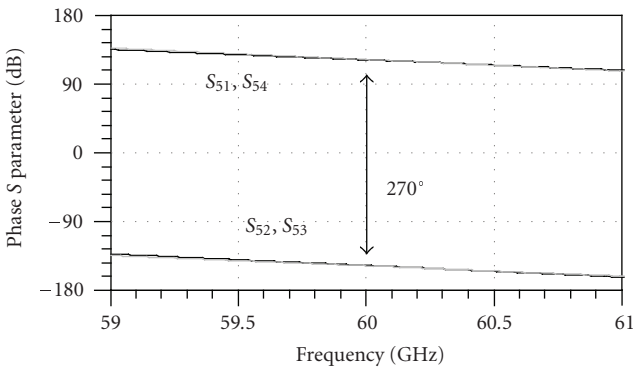


FIGURE 5: Simulation results of the transmission S parameter phase corresponding to the LO input.

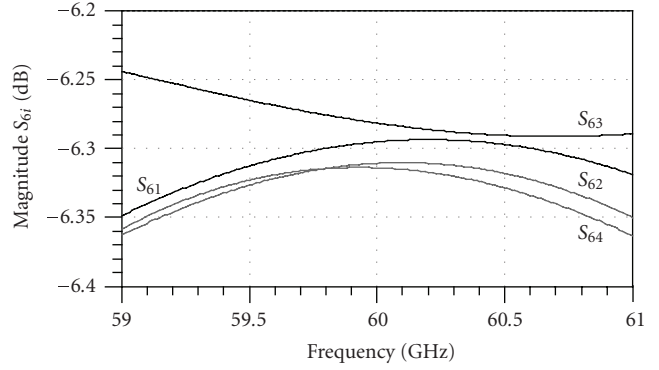


FIGURE 7: Simulation results of  $S_{6i}$  magnitudes at RF input.

Figure 4 shows simulation results of S parameters at RF input ports of the proposed multipoint circuit. Excellent return losses and isolation between RF inputs were obtained in a 2 GHz frequency band centered at the 60 GHz operating frequency (return loss less than 20 dB).

The phase and the magnitude of the transmission S parameters are also of main interest to obtain the requested four “ $q_i$  points” of the multipoint circuit (see the block diagram of Figure 1). Figures 5 and 6 show the phase of transmission scattering parameters between inputs and outputs versus the frequency. The phases of these parameters are shifted by  $90^\circ$  multiples over the frequency band, as suggested in the block diagram.

As suggested in previous figures, the use of the V-band couplers allows  $90^\circ$  phase difference over a very wide band, suitable for a high-quality I/Q mixer.

Figure 7 shows the magnitude of transmission S parameters between the RF input port and the four outputs. Compared to the ideal multipoint model, a supplementary loss of around 0.3 dB appears at the central frequency. Similar results related to the magnitude of transmission S parameters between the LO input port and the four outputs are also obtained.

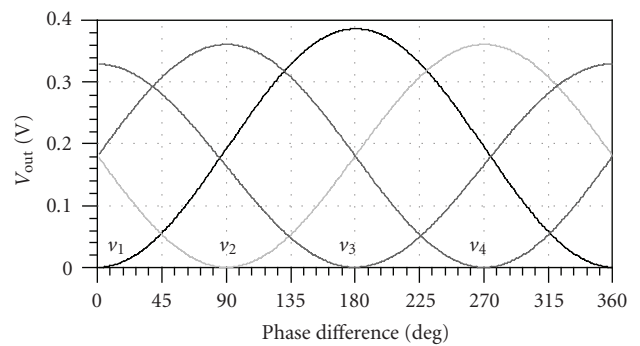


FIGURE 8: Simulation results of  $V_{out}$  versus inputs phase difference.

In order to demonstrate that the multipoint is a four “ $q_i$ -point” circuit having all points spaced by  $90^\circ$ , a harmonic balance simulation was performed at 60 GHz using a multipoint model based on ADS momentum S parameter results. Power detectors were connected at the four outputs. The phase difference between millimeter-wave inputs was swept in a  $360^\circ$  range and the RF input signal power was set to 0 dBm. The multipoint output detected voltages versus the phase difference are shown in Figure 8.

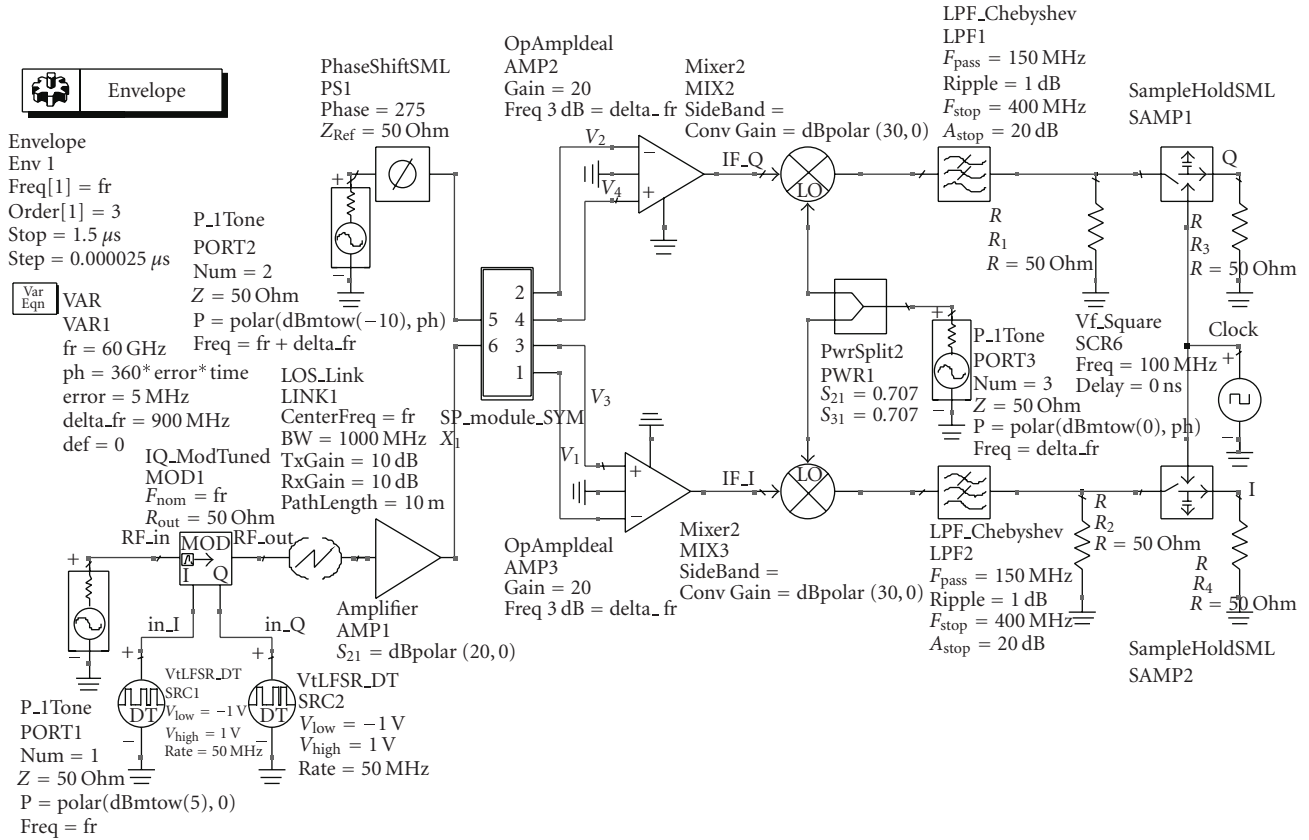


FIGURE 9: ADS simulation block diagram of the multiport heterodyne receiver.

As seen, the output voltage minimum values are shifted by  $90^\circ$  multiples as requested for this multiport architecture. In addition, the output voltages at ports 1 and 3 and at ports 2 and 4, respectively, are in antiphase, as demonstrated in the theoretical part (see (3) and (4)). Therefore I/Q output signals can be obtained according to (5) using two differential amplifiers.

### 3. DEMODULATION RESULTS

Demodulation results of the V-band multiport heterodyne receiver are presented in this section.

The multiport heterodyne receiver simulation block diagram, using ADS software, is presented in Figure 9. Simulations are performed using a 60 GHz carrier frequency of a MPSK/QAM modulated signal. According to the proposed datarate of 100–400 Mbps, the IF of the heterodyne receiver was chosen at 900 MHz. The second frequency conversion using conventional mixers is also implemented.

As presented in the same figure, the proposed multiport heterodyne receiver is composed, as usually, of RF, IF, and baseband stages. The V-band RF front-end contains the low-noise amplifier AMP1 and the V-band I/Q mixer (the V-band multiport module including four power detectors).

Excluding the IF differential amplifiers (AMP2 and AMP3), the IF and baseband stages have a conventional architecture: IF down-converters (MIX2, MIX3, LPF1, and

LPF2) and sample-and-hold circuits (SAMP1 and SAMP2). Baseband amplifiers can be used to improve the overall gain of the receiver.

In order to obtain the signal waveforms or spectrums, an ADS envelope simulation at the operating frequency of 60 GHz is performed using the simulation diagram of Figure 9. In this diagram a 100 Mbps QPSK pseudorandom signal is generated at the transmitter using two generators connected to the I/Q modulator.

Various MPSK/QAM modulations will be also analyzed in this work using the ADS vector modulator model. It is noted that a loss-link model based on Friis equation is used to simulate the free-space signal propagation.

Figure 10 shows the typical IF spectrum (IF\_I or IF\_Q signals) using the proposed architecture and the same QPSK signal of 100 Mbps. As well known, and as this spectrum suggested, a 400 Mbps QPSK signal can be demodulated using the same IF of 900 MHz. However, the bandwidth of the IF stage must be increased according to the new datarate.

The same architecture can also meet all high-speed requirements of the IEEE 802.15.3c wireless standard using an increased IF. For this purpose, the IF differential amplifiers based on operational amplifiers must be replaced by differential amplifiers using microwave transistors.

Figure 11 shows a typical spectrum of a baseband quadrature signal (I or Q) obtained after the second down-conversion and the sample-and-hold circuit (SHC). We note

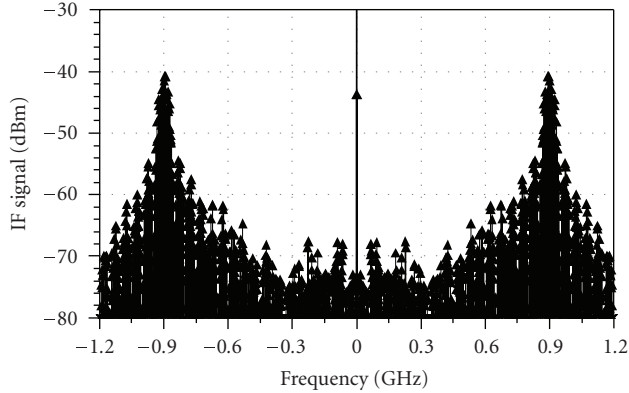


FIGURE 10: Typical spectrum of the IF signal.

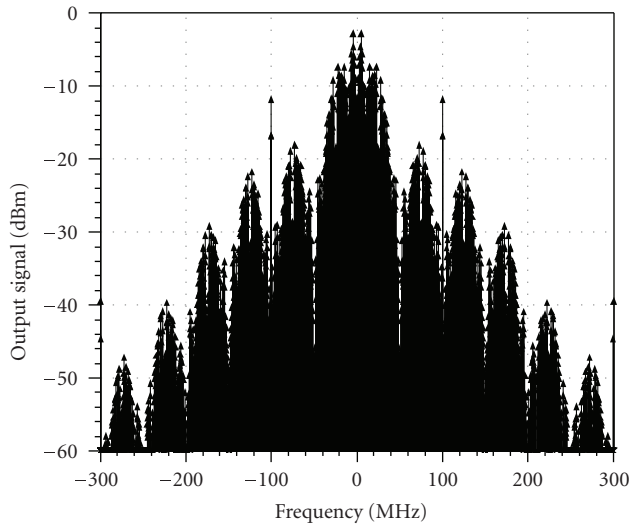


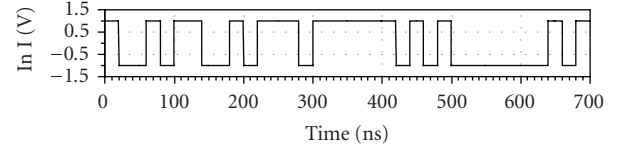
FIGURE 11: Typical spectrum of a baseband quadrature signal.

that the spectral lines of  $\pm 100$  MHz represent the clock signal of the SHC.

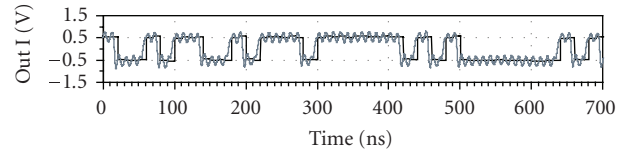
A pseudorandom bit sequence of 700 nanoseconds is represented in Figure 12. As seen, the demodulated output signals have the same bit sequence as those generated by the transmitter. The gray line corresponds to the baseband signal before the sample-and-hold circuit which dramatically improves the demodulated signal shape.

The demodulation results demonstrate the validity of the proposed heterodyne architecture. Bit error rate (BER) analysis is also performed in this work using an appropriated length pseudorandom bit-stream.

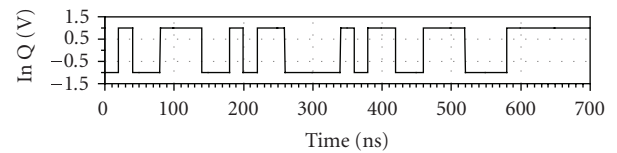
Figure 13 shows all possible 16 states of the I/Q output signals corresponding to a 16 QAM modulation. As seen, each signal has four different levels corresponding to the signal constellation. These levels are quasi-equidistant and symmetrical versus the zero voltage level. The gray line has the same signification as in the previous figure. Therefore, the SHC improves the demodulation results, as expected.



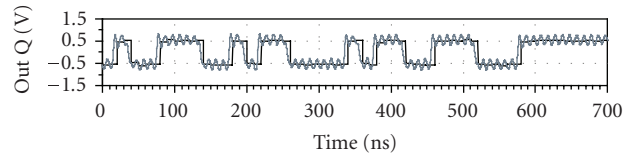
(a)



(b)



(c)



(d)

FIGURE 12: Demodulation results of 100 Mb/s QPSK pseudorandom bit sequence.

Supposing a perfect synchronism and no additional noise, Figure 14 shows various simulation results of demodulated constellations using the proposed heterodyne architecture for high-speed MPSK/QAM signals: 100 Mbps for QPSK, 200 Mbps for 8PSK and 16 QAM, and 400 Mbps for 16PSK.

As seen, all clusters of demodulated constellations are very well positioned and individualized. Due to the differential approach and the multiport design, the DC offset represented by the distance between the central point and the origin is almost zero.

Figure 15 shows the demodulation results of a 16 QAM signal for a low signal to noise ratio of 5 dB (a white noise was added in the transmission path). Simulation results show that all clusters remain well individualized and well positioned in the I/Q complex plan. Furthermore, signal processing techniques will allow to obtain improved demodulation results.

As known, a millimeter-wave oscillator does not have excellent frequency stability and is difficult to be controlled. If the difference between the carrier and the local oscillator is not exactly equal to IF, the demodulated constellation turns clockwise or anti-clockwise, depending on the sign of this

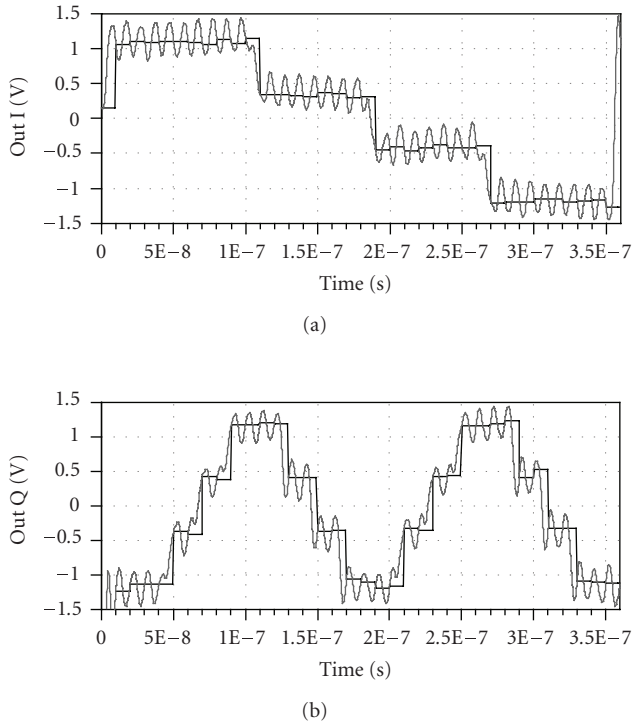


FIGURE 13: Demodulation results of 16 QAM signal.

difference [9]. Figure 16 shows a 16 QAM constellation in the case of  $45^\circ$  phase error of synchronism of the millimeter-wave oscillator. However, these frequency/phase errors can be successfully compensated using signal processing techniques. The second LO must be dynamically adjusted by a control loop.

Figure 17 shows the BER versus the energy per bit to the spectral noise density ( $E_b/N_0$ ) for various millimeter-wave LO frequency errors (no error, 5 MHz, and 25 MHz, resp.). The frequency/phase error compensation technique of the second LO in the case of a 100 Mbps QPSK modulated signal is used. Simulation shows an excellent result for the proposed receiver. The BER is less than  $10^{-6}$  for an  $E_b/N_0$  ratio of 12 dB, considering the specified frequency errors of synchronism of the millimeter-wave oscillator.

The heterodyne architecture will allow an increased gain of the receiver for relatively high range applications compared to the homodyne architecture. Simulation results show more than 70 dB of the multiport heterodyne receiver overall gain, compared to 50 dB of gain, reported for the homodyne receivers [6, 7].

#### 4. CONCLUSIONS

Simulation results of a V-band millimeter-wave multiport heterodyne receiver have been presented in this paper. The millimeter-wave frequency conversion is obtained using the specific properties of the multiport circuit, avoiding the use of a costly conventional active mixer.

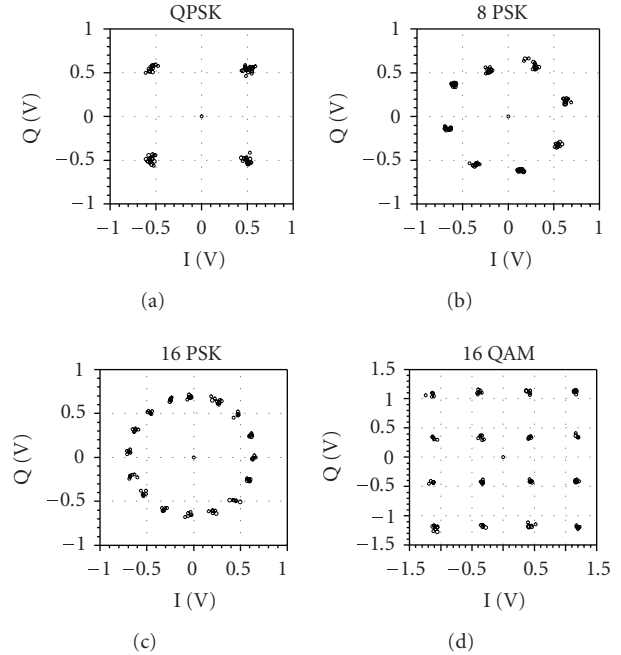


FIGURE 14: Demodulated high-speed MPSK/QAM signals.

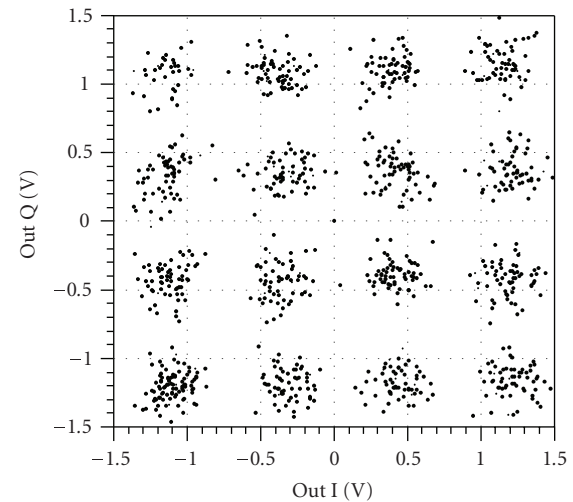


FIGURE 15: Constellation of demodulated 16 QAM signal in presence of a white noise.

Excellent demodulation results were obtained using high-speed V-band MPSK/QAM modulated signals. Simulated BER results, in the case of an important millimeter-wave LO frequency error from synchronism (dynamically compensated using the second LO), are excellent. Compared to the direct conversion, due to the heterodyne architecture, an improved overall gain was obtained.

The proposed multiport heterodyne architecture enables the design of compact and low-cost wireless millimeter-wave communication receivers for future high-speed wireless communication systems, according to the IEEE 802.15.3c wireless standard.

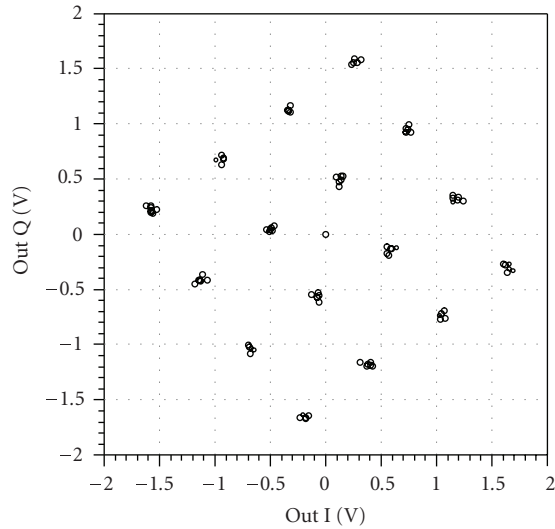


FIGURE 16: Constellation of demodulated 16 QAM signal in the case of  $45^\circ$  phase error of synchronism.

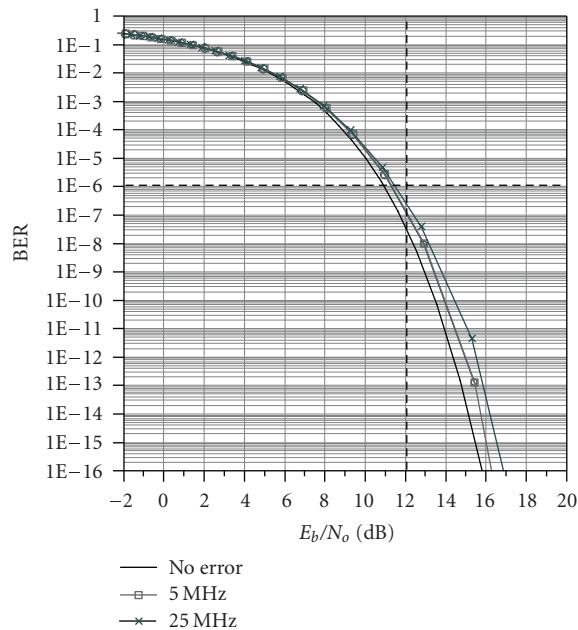


FIGURE 17: BER simulation results for various errors of synchronism of the millimeter-wave oscillator.

## ACKNOWLEDGMENT

The financial support of the National Science Engineering Research Council (NSERC) of Canada is gratefully acknowledged.

## REFERENCES

- [1] P. Smulders, "Exploiting the 60 GHz band for local wireless multimedia access: prospects and future directions," *IEEE Communications Magazine*, vol. 40, no. 1, pp. 140–147, 2002.
- [2] J. Wenger and J. Splettstoesser, "Ka- and V-band MMIC components for personal communication networks," in *Proceedings of IEEE MTT-S International Microwave Symposium Digest*, vol. 2, pp. 491–494, San Francisco, Calif, USA, June 1996.
- [3] A. Nestic, I. Radnovic, and V. Brankovic, "Ultra-wide band printed antenna array for 60 GHz frequency range," in *Proceedings of IEEE Antennas and Propagation Society International Symposium Digest*, vol. 2, pp. 1272–1275, Montreal, Quebec, Canada, July 1997.
- [4] K. S. Ang, M. Chongcheawchamnan, and I. D. Robertson, "Monolithic resistive mixers for 60 GHz direct conversion receivers," in *Proceedings of IEEE Radio Frequency Integrated Circuits Symposium, Digest of Papers (RFIC '00)*, pp. 35–38, Boston, Mass, USA, June 2000.
- [5] T. Brabetz and V. Fusco, "Six-port receiver MMIC for V-band MBS applications," in *Proceedings of the 11th Gallium Arsenide Applications Symposium (GAAS '03)*, pp. 97–99, Munich, Germany, October 2003.
- [6] S. O. Tatu, E. Moldovan, K. Wu, and R. G. Bosisio, "A new direct millimeter-wave six-port receiver," *IEEE Transactions on Microwave Theory and Techniques*, vol. 49, no. 12, pp. 2517–2522, 2001.
- [7] S. O. Tatu, E. Moldovan, G. Brehm, K. Wu, and R. G. Bosisio, "Ka-band direct digital receiver," *IEEE Transactions on Microwave Theory and Techniques*, vol. 50, no. 11, pp. 2436–2442, 2002.
- [8] S. O. Tatu, E. Moldovan, K. Wu, R. G. Bosisio, and T. A. Denidni, "Ka-band analog front-end for software-defined direct conversion receiver," *IEEE Transactions on Microwave Theory and Techniques*, vol. 53, no. 9, pp. 2768–2776, 2005.
- [9] S. O. Tatu and T. A. Denidni, "Millimeter-wave six-port heterodyne receiver concept," in *Proceedings of IEEE Microwave Theory and Techniques Symposium Digest*, pp. 1999–2002, San Francisco, Calif, USA, June 2006, Conference CD, IEEE Catalogue Number 06CH37734C.
- [10] S. O. Tatu and E. Moldovan, "Alternative millimeter-wave communication receivers in six-port technology," in *Proceedings of Canadian Conference on Electrical and Computer Engineering (CCECE '06)*, Ottawa, Canada, May 2006.